ELSEVIER

17 November 1997

PHYSICS LETTERS A

Physics Letters A 235 (1997) 499–503

Semiconductor lasers and Kolmogorov spectra

Yuri V. Lvov [a,b], Alan C. Newell [a,c]

[a] *Department of Mathematics, University of Arizona, Tucson, AZ 85721 USA*
[b] *Department of Physics, University of Arizona, Tucson, AZ 85721, USA*
[c] *Mathematical Institute, University of Warwick, Coventry CV4 7AL, UK*

Received 25 June 1997; accepted for publication 14 August 1997
Communicated by A.P. Fordy

Abstract

We make a prima facie case that there could be distinct advantages to exploiting a new class of finite flux equilibrium solutions of the quantum Boltzmann equation in semiconductor lasers. © 1997 Published by Elsevier Science B.V.

1. Introduction

At first sight, it may very well seem that the two subjects linked in the title have little in common. What do semiconductor lasers have to do with behavior normally associated with fully developed hydrodynamic turbulence? In order to make the connection, we begin by reviewing the salient features of semiconductor lasers. In many ways, they are like two level lasers in that the coherent light output is associated with the in phase transitions of an electron from a higher to lower energy state. In semiconductors, the lower energy state is the valence band from which sea electrons are removed leaving behind positively charged holes. The higher energy state is the conduction band. The quantum of energy released corresponds to an excited electron in the conduction band combining with a hole in the lower band below the bandgap. Bandgaps, or forbidden energy zones are features of the energy spectrum of an electron in periodic potentials introduced in this case by the periodic nature of the semiconductor lattice.

However, there are two important ways in which the semiconductor laser differs from and is more complicated than the traditional two-level laser model. First, there is a continuum of bandgaps parameterized by the electron momentum $\boldsymbol{k}$ and the laser output is a weighted sum of contributions from polarizations corresponding to electron–hole pairs at each momentum value. In this feature, the semiconductor laser resembles an inhomogeneously broadened two level laser. Second, electrons and holes interact with each other via Coulomb forces. Although this interaction is screened by the presence of many electrons and holes, it is nonetheless sufficiently strong to lead to a nonlinear coupling between electrons and holes at different momenta. The net effect of these collisions is a redistribution of carriers (the common name for both electrons and holes) across the momentum spectrum. In fact it is the fastest ($\approx$ 100 fs) process (for electric field pulses of duration greater than picoseconds) and because of this, the gas of carriers essentially relaxes to a distribution corresponding to an equilibrium of this collision process. This equilibrium state is commonly taken to be that of thermodynamic equilibrium for fermion gases, the Fermi–Dirac distribution char-

0375-9601/97/$17.00 © 1997 Published by Elsevier Science B.V. All rights reserved.
PII S0375-9601(97)00656-7

acterized by two parameters, the chemical potential μ and temperature T, slightly modified by the presence of broadband pumping and damping.

But the Fermi–Dirac distribution is not the only equilibrium of the collision process. There are other stationary solutions, called finite flux equilibria, for which there is a finite and constant flux of carriers and energy across a given spectral window. The Fermi–Dirac solution has zero flux of both quantities. It is the aim of this Letter to suggest that these finite flux equilibria are more relevant to situations in which energy and carriers are added in one region of the spectrum, redistributed via collision processes to another region where they are absorbed. Moreover, it may be advantageous to pump the laser in this way because such a strategy may partially overcome the deleterious effects of Pauli blocking. The Pauli exclusion principle means that two electrons with the same energy and spin cannot occupy the same state at a given momentum. This leads to inefficiency because the pumping is effectively multiplied by a factor $1 - n_s(\boldsymbol{k})$, $s = e, h$ for electrons and holes respectively, denoting the probability of not finding an electron (hole) in a certain $\boldsymbol{k}$ (used to denote both momentum and spin) state. But, near the momentum value corresponding to the lasing frequency ω_L, $n_s(\boldsymbol{k})$ is large ($n_e(\boldsymbol{k}) + n_h(\boldsymbol{k})$ must exceed unity) and Pauli blocking significant. Therefore, pumping the laser in a window about $\omega_0 > \omega_L$ in such a way that one balances the savings gained by lessening the Pauli blocking (because the carriers density $n_s(\boldsymbol{k})$ decreases with $k = |\boldsymbol{k}|$) with the extra input energy required (because k is larger), and then using the finite flux solution to transport carriers (and energy) back to lasing frequency, seems an option worth considering. The aim of this Letter is to demonstrate, using the simplest possible model, that this alternative is viable. More detailed results using more sophisticated (but far more complicated) models will be given later.

These finite flux equilibria are the analogies of the Kolmogorov spectra associated with fully developed, high Reynolds number hydrodynamic turbulence and the wave turbulence of surface gravity waves on the sea. In the former context, energy is essentially added at large scales (by stirring or some instability mechanism), is dissipated at small (Kolmogorov and smaller) scales of the order of less than the inverse three quarter power of the Reynolds number.

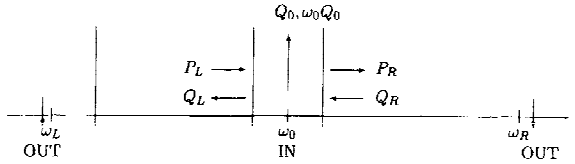

Fig. 1. Carriers and energy are added at ω_0 at rates Q_0 and $\omega_0 Q_0$. Energy and some carriers are dissipated at $\omega_R > \omega_0$ (an idealization) and carriers and some energy are absorbed by the laser at ω_L. (The carriers number will build until the laser switches on.) A little calculation shows $Q_L = Q_0(\omega_R - \omega_0)/(\omega_R - \omega_L)$, $Q_R = Q_0(\omega_L - \omega_0)/(\omega_R - \omega_L)$, $P_R = Q_0\omega_R(\omega_0 - \omega_L)/(\omega_R - \omega_L)$, and $P_L = \omega_L Q_0(\omega_0 - \omega_R)/(\omega_R - \omega_L)$. Finite flux stationary solutions are realized in the windows (ω_L, ω_0) and (ω_0, ω_R) although in practice there will be some losses through both these regions.

It cascades via nonlinear interactions from the large scales to the small scales through a window of transparency (the inertial range in which neither forcing nor damping is important) by the constant energy flux Kolmogorov solution. Indeed, for hydrodynamic turbulence, the analogue to the Fermi–Dirac distribution, the Rayleigh–Jeans spectrum of equipatitions, is irrelevant altogether. The weak turbulence of surface gravity waves is the classical analogue of the case of weakly interacting fermions. The mechanism for energy and carrier density (particle number) transfer is "energy" and "momentum" conserving binary collisions satisfying the "four wave resonance" conditions

$$\begin{aligned} &\boldsymbol{k} + \boldsymbol{k}_1 = \boldsymbol{k}_2 + \boldsymbol{k}_3, \\ &\omega(\boldsymbol{k}) + \omega(\boldsymbol{k}_1) = \omega(\boldsymbol{k}_2) + \omega(\boldsymbol{k}_3). \end{aligned} \tag{1}$$

In the semiconductor context, $\hbar\omega(\boldsymbol{k}) = \hbar\omega_{\text{gap}} + \epsilon_e(\boldsymbol{k}) + \epsilon_h(\boldsymbol{k})$ (which can be well approximated by $\alpha + \beta k^2$), where $\hbar\omega_{\text{gap}} = \epsilon_{\text{gap}}$ corresponds to the minimum bandgap and $\epsilon_e(\boldsymbol{k})$, $\epsilon_h(\boldsymbol{k})$ are electron and hole energies. In each case, there is also a simple relation $E(\boldsymbol{k}) = \omega n(\boldsymbol{k})$ between the spectral energy density $E(\boldsymbol{k})$ and carrier (particle number) density $n(\boldsymbol{k})$. As a consequence of conservation of both energy and carriers, it can be argued (schematically shown in Fig. 1 and described in its caption), that the flux energy (and some carriers) from intermediate momentum scales (around k_0 say) at which it is injected, to higher momenta (where it is converted into heat) must be accompanied by the flux of carriers and some energy from k_0 to lower momenta at which it will be absorbed by the laser. It is the latter solution that we plan to exploit.

2. Model

We present the results of a numerical simulation of a greatly simplified model of semiconductor lasing in which we use parameter values which are realistic but make fairly severe approximations in which we (a) assume that the densities of electrons and holes are the same (even though their masses differ considerably), (b) ignore carrier recombination losses and (c) model the collision integral by a differential approximation [1–3] in which the principal contributions to wavevector quartets satisfying (1) are assumed to come from nearby neighbors. Despite the brutality of the approximations, the results we obtain are qualitatively similar to what we obtain using more sophisticated and complicated descriptions.

The semiconductor Maxwell–Bloch equations are [4,5]

$$\frac{\partial e}{\partial t} = \mathrm{i}\frac{\Omega}{2\epsilon_0}\int \mu_k p_k \,\mathrm{d}\boldsymbol{k} - \gamma_E e, \tag{2}$$

$$\frac{\partial p_k}{\partial t} = (\mathrm{i}\Omega - \mathrm{i}\omega_k - \gamma_P)p_k - \frac{\mathrm{i}\mu_k}{2\hbar}(2n_k - 1)e, \tag{3}$$

$$\frac{\partial n_k}{\partial t} = \Lambda(1 - n_k) - \gamma_k n_k + \left(\frac{\partial n_k}{\partial t}\right)_{\text{collision}} - \frac{\mathrm{i}}{2\hbar}\left(\mu_k p_k e^* - \mu_k p_k^* e\right). \tag{4}$$

Here $e(t)$ and $p_k(t)$ are the electric field and polarization at momentum $\boldsymbol{k}$ envelopes of the carrier wave $\exp(-\mathrm{i}\Omega t + \mathrm{i}\bar{K}z)$, where Ω is the cavity frequency (we assume single mode operation only) and $n(k)$ is the carrier density for electrons and holes. The constants γ_E, γ_P are model electric field and homogeneous broadening losses, ϵ_0 is the dielectric constant, μ_k is the weighting accorded to different $\boldsymbol{k}$ momentum (modeled by $\mu_k = \mu_{k=0}/(1 + \epsilon_k/\epsilon_{\text{gap}})$), Λ_k and γ_k represent carrier pumping and damping. In (4), the collision term is all important and is given by

$$\frac{\partial}{\partial t}n_k = 4\pi\int |T_{kk_1k_2k_3}|^2[n_{k_2}n_{k_3}(1 - n_{k_1} - n_k) + n_k n_{k_1}(n_{k_2} + n_{k_3} - 1)] \times \delta(\boldsymbol{k} + \boldsymbol{k}_1 - \boldsymbol{k}_2 - \boldsymbol{k}_3) \times \delta(\omega_k + \omega_{k_1} - \omega_{k_2} - \omega_{k_3})\,\mathrm{d}\boldsymbol{k}_1\,\mathrm{d}\boldsymbol{k}_2\,\mathrm{d}\boldsymbol{k}_3, \tag{5}$$

where $T_{kk_1k_2k_3}$ is the coupling coefficient measuring mutual electron and hole interactions. We make the weak assumption that all fields are isotropic and make a convenient transformation from k ($= |\boldsymbol{k}|$) to ω via the dispersion relation $\omega = \omega(\boldsymbol{k})$ defining the carrier density N_ω by $\int N_\omega \,\mathrm{d}\omega = \int n(\boldsymbol{k})\,\mathrm{d}\boldsymbol{k}$ or $N_\omega = 4\pi k^2\,\mathrm{d}k/(\mathrm{d}\omega)n(\boldsymbol{k})$. Then, in the differential approximation, (5) can be written as both,

$$\frac{\partial N_\omega}{\partial t} = \frac{\partial^2 K}{\partial \omega^2}, \quad \frac{\partial \omega N_\omega}{\partial t} = -\frac{\partial}{\partial \omega}\left(K - \omega\frac{\partial K}{\partial \omega}\right), \tag{6}$$

with

$$K = -I\omega^s[n_\omega^4(n_\omega^{-1})'' + n_\omega^2(\ln n_\omega)''],$$
$$n_\omega = n(\boldsymbol{k}(\omega)),$$

where a prime denotes $\partial/\partial\omega$, s is the number computed from the dispersion relation, the dependence of $T_{kk_1k_2k_3}$ on $\boldsymbol{k}$ and dimensions (s is of the order of 7 for semiconductors.) The conservation forms of the equations for N_ω and $E_\omega = \omega N_\omega$ allow us to identify $Q = \partial K/\partial\omega$ (positive if carriers flow from high to low momenta) and $P = K - \omega\,\partial K/\partial\omega$ (positive if energy flows from low to high momenta) as the fluxes of carriers and energy, respectively. Moreover, the equilibrium solutions are now all transparent. The general stationary solution of (6) is the integral of $K = Q\omega + P$ which contains four parameters, two (chemical potential and temperature) associated with the fact that K is a second derivative, and two constant fluxes Q and P of carriers and energy. The Fermi–Dirac solution $n_\omega = [\exp(A\omega + B) + 1]^{-1}$, the solution of $K = 0$, has zero flux. We will now solve (2), (3) and (4) after angle averaging (4) and replacing $(4\pi k^2\,\partial k/\partial\omega)(\partial n_k/\partial\omega)_{\text{collision}}$ by $\partial^2 K/\partial\omega^2$. The value of the constant I is chosen to ensure that solutions of (6) relax in a time of 100 fs.

3. Results

We show the results in Figs. 2, 3, and 4. First, to the test accuracy, we show, in Fig. 2, the relaxation of (6) to a pure Fermi–Dirac spectrum in the window $\omega_L = 1 < \omega < \omega_0 = 2$. The boundary conditions correspond to $P = Q = 0$ at both ends. We then modify boundary conditions to read $Q = Q_0 > 0$ and $P = 0$ at both ends. Next, in Figs. 3 and 4, we show the results of two experiments in which we compare the efficiencies of two experiments in which we arrange to

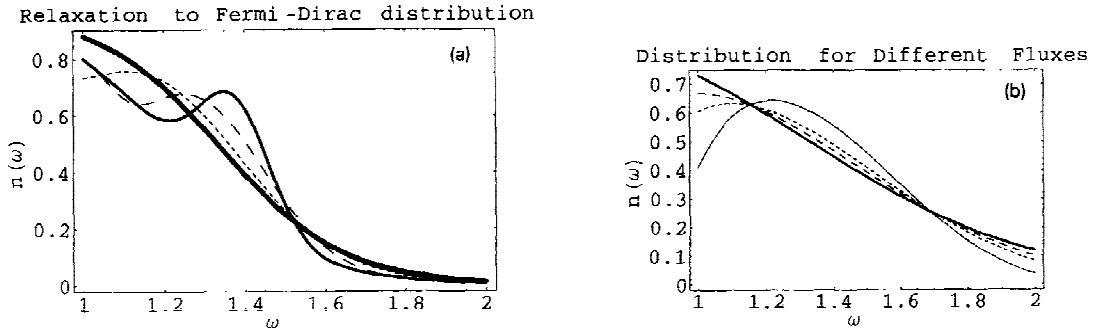

Fig. 2. To test the accuracy we take some initial distribution function (thin line) and plot its time evolution as described by (6) with boundary conditions $P = Q = 0$ at both ends. The distribution function relaxes to the Fermi–Dirac state (thick line). Several intermediate states are shown by long-dashed and short-dashed lines (a). We then modify the boundary conditions to $P = 0$, $Q = Q_0 > 0$ at both ends. Then the initial distribution function (thick line) relaxes to finite-Q-equilibria as shown by a long-dashed line. We then change the boundary conditions to $P = 0, Q = Q_1 > Q_0$ at both ends, so that the distribution function is shown by a short-dashed line. Increasing Q at the boundaries even further, so that $P = 0, Q = Q_2 > Q_1$ at both ends, the distribution function is given by a dotted line (b)

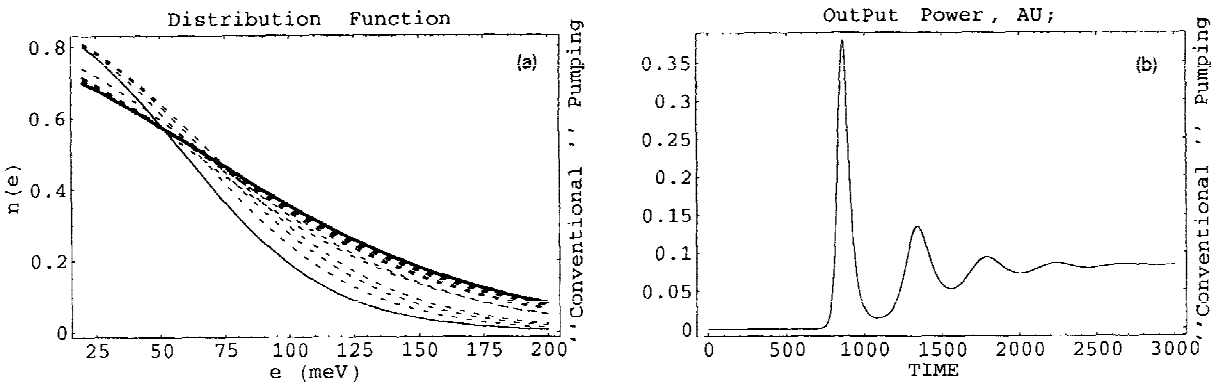

Fig. 3. We now solve (2)–(4) with the collision term given by (6). We pump broadly, so that the effective carrier distribution has a zero flux. The initial distribution function (thin line) builds up because of a global pumping (dashed lines), until the laser switches on. The final (steady) distribution function is shown by a thick solid line (a). The output power (in arbitrary units) as a function of time (measured in relaxation times $\simeq$ 100 fs) is also shown (b).

(i) pump broadly so that the effective carrier distribution equilibrium has zero flux and (ii) pump carriers and energy into a narrow band of frequencies about ω_0 and simulate this by specifying carrier and energy flux rates Q_L and $P_L = -\omega_L Q_L$ (P_L chosen so that the energy absorbed by the laser is consistent with the number of carriers absorbed there) at the boundary $\omega = \omega_0$. $\omega = \omega_L$ is the frequency at which the system lases.

In both cases, the rate of addition of carriers and energy is (approximately) the same. The results support the idea that it is worth exploring the exploitation of the finite flux equilibrium. The carrier density of the equilibrium solutions at ω_0 is small thus making pumping more efficient there. The output of the laser is greater by a factor of 10. While we do not claim that, when all effects are taken account of, this advantage will necessary remain, we do suggest that the strategy of using finite flux equilibrium solutions of the quantum Boltzmann equation is worth further exploration.

Acknowledgement

The authors wish to thank the Arizona Center for Mathematical Sciences (ACMS) for support. ACMS is sponsored by AFOSR contract F49620-97-1-0002 and 94-1-0144-DEF under the University Research Initiative Program at the University of Arizona, Department of Mathematics.

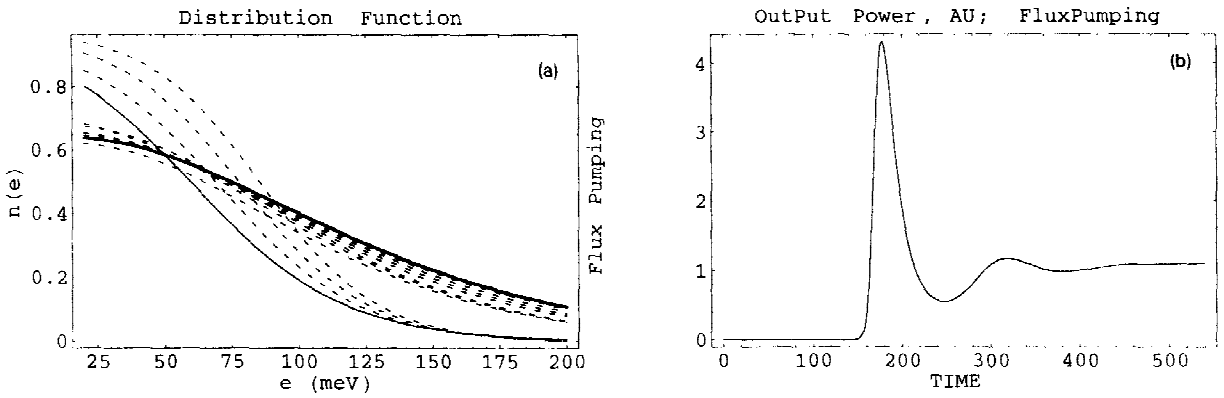

Fig. 4. We pump in the narrow region around $\omega_0 \simeq 200\,\text{meV}$ and we model this by specifying carrier and energy flux rates Q_L and $P_L = -\omega_L Q_L$. The initial distribution function (thin line) builds up because of the influx of particles and energy from the right boundary (dashed lines), until the laser switches on. The final (steady) distribution function is shown by a thick solid line and corresponds to a flux of particles and energy from the right boundary (where we add particles and energy) to the left boundary, where the system lases (a). The output power as a function of time is also shown (b).

References

[1] S. Dyachenko, A.C. Newell, A. Pushkarev, V.E. Zakharov, Physica D 57 (1992) 96.

[2] S. Hasselmann, K. Hasselmanm, J.H. Allender, T.P. Barnett, J. Phys. Oceonography 15 (1985) 1378.

[3] V.E. Zakharov, V.S. L'vov, G. Falkovich, Kolmogorov Spectra of Turbulence (Springer, Berlin, 1992).

[4] W.W. Chow, S.W. Koch, M. Sargent, Semiconductor Laser Physics (Springer, Berlin, 1994).

[5] H. Haug, S.W. Koch, in: Quantum Theory of the Optical and Electronic Properties of the Semiconductors (World Scientific, Singapore, 1990).